2-1-1996

EFFICENT USE OF NARROWBAND RADIO CHANNELS FOR MOBILE DIGITAL COMMUNICATIONS

Michael P. Fitz
Purdue University School of Electrical and Computer Engineering

James V. Krogmeier
Purdue University School of Electrical and Computer Engineering

Jimm Grimm
Purdue University School of Electrical and Computer Engineering

Tai Ann Chen
Purdue University School of Electrical and Computer Engineering

Tim Magnusen
Purdue University School of Electrical and Computer Engineering

See next page for additional authors

Efficient Use of Narrowband Radio Channels For Mobile Digital Communications

Michael P. Fitz
James V. Krogmeier
Jimm Grimm
Tai-Ann Chen
Tim Magnusen
Jerome Gansman

TR-ECE 96-2
February 1996

School of Electrical
and Computer Engineering
Purdue University
West Lafayette, Indiana 47907-1285

EFFICIENT USE OF NARROWBAND RADIO CHANNELS FOR MOBILE DIGITAL COMMUNICATIONS

Michael P. Fitz, James V. Krogmeier, Jimm Grimm, Tai-Ann Chen, Tim Magnusen and Jerome Gansman
Purdue University, West Lafayette, Indiana

Wen-Yi Kuo, AT&T Bell Laboratories

School of Electrical Engineering
1285 Electrical Engineering Building
Purdue University
West Lafayette, In 47907-1285

Funded by
the IDEA Program
of the Transportation Research Board,
National Academy of Science

Table of Contents

List of Figures

List of Tables

Abstract

The Intelligent Transportation System (ITS) relies heavily on data communications systems to link field equipment such as traffic sensors, changeable message signs and incident response vehicles with traffic operations centers. The Federal Highway Administration (FHWA) has received an allocation of five channels in the 220 MHz band to provide a communications resource for ITS applications. This report investigates a high efficiency mobile wireless modem with a spectral efficiency of 3 bps/Hz. The modem incorporates the following techniques to compensate for the fading channel: transmitter antenna diversity, modulation using intentional frequency offset, interleaved block codes, symbol timing and frame synchronization optimized for fading channels, soft decision decoding optimized for fading, and pilot symbol assisted modulation (PSAM) channel estimation.

A prototype of this wireless modem has been constructed and subjected to full bench testing. Preliminary field testing has been performed and more is in progress.

EFFICIENT USE OF NARROWBAND RADIO CHANNELS FOR MOBILE DIGITAL COMMUNICATIONS

ITS-IDEA Project 15

Michael P. Fitz, James V. Krogmeier, Jimm Grimm, Tai-Ann Chen, Tim Magnusen and Jerome Gansman
Purdue University, West Lafayette, Indiana
Wen-Yi Kuo, AT&T Bell Laboratories

EXECUTIVE SUMMARY

Data communications systems linking field equipment such as traffic sensors, changeable message signs and incident response vehicles with traffic operations centers are a fundamental requirement of Federal Highway Administration (FHWA) plans for deployment of Intelligent Transportation System (ITS) traffic management and traveler information services. The FHWA has received an allocation of five channels in the 220 MHz band to provide a communications resource for ITS applications.

High efficiency modems will be required to make maximum beneficial use of the ITS 220 MHz channels *given* the limited available bandwidth and the challenge of a mobile radio channel. The design of highly bandwidth efficient modems for wireless mobile data transmission is much more difficult than the design of wireline modems of similar spectral effioiency. The combination of motion and multipath transmission in the mobile channel introduces challenging impairments which require a more sophisticated modem design. Together, multipath transmission and receiver or transmitter motion produce a fading signal characteristic which is the predominant impairment for narrowband wireless communications (See Figure 1). The best spectral efficiencies currently available for the land mobile data communications (fading) channel are about 1 bit per second (bps) per Hz whereas wireline modems are available which achieve a transmission rate of 28.8 kbps in a 3.2 kHz telephone circuit (no fading) for an efficiency of 9 bps/Hz. It is possible to improve the efficiency of wireless modems with a more sophisticated modem design.

The product resulting from this IDEA project is a wireless motlem architecture that provides bandwidth efficient data communications in the 220 MHz ITS spectral allocations. The goal is to provide greater than 12 kbps transmission capacity on the 4 kHz channels (3 bps/Hz spectral efficiency) for mobile applications. This work has resulted in a proof of concept of a general purpose resource for data comrnunications in traffic management systems, traveler information systems, and/or commercial vehicle operations. The system was verified by a rigorous theoretical performance analysis, bench testing and indoor field testing. Field tests in mobile urban environments are planned this spring in Indianapolis and Lafayette. The main features of the system designed in this project are: (1) 3571 Hz symbol rate and 4000 Hz bandwidth, (2) quadrature amplitude modulation (QAM), (3) pilot symbol assisted modulation, (4) forward error control coding (FEC), (5) transmitter antenna diversity, and (6) synchronization optimized for fading, The novel features in the design of the modem which greatly enhance its performance in the fading channel are

1. pilot symbol assisted modulation which provides compensation for fading via channel estimation,
2. transmitter antenna diversity with intentional frequency offset which allows a principled use of interleaving coupled with forward error control coding, and
3. synchronization optimized for fading channels.

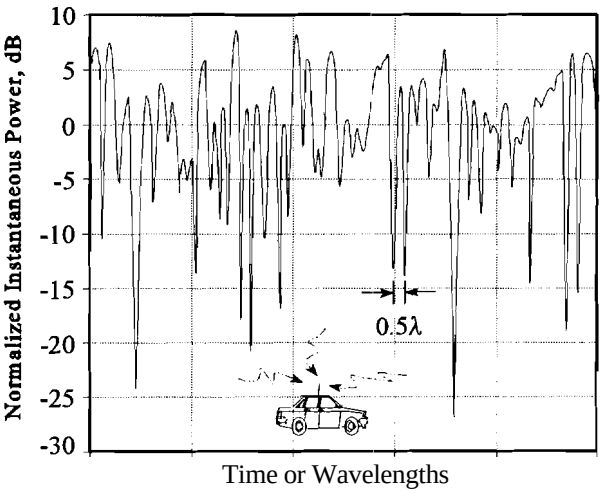

Figure 1: Typical fading channel magnitude

The system is implemented using the combination of a digital signal processor, discrete electronics, and high level software. The special features of the chosen architecture are

1. all sophisticated signal processing is implemented in software which provides both high performance and flexibility, and

2. the system forms an ideal testbed for testing of the design of future enhancements and modifications to fit specific ITS applications.

Transmitter and receiver block diagrams for the wireless modem produced by this project are shown in Figures 9 and 10, respectively. Each block in the transmitter works in conjunction with a block in the receiver (e.g., the FEC coder and the FEC decoder, the interleaver and the de-interleaver, etc.)

On the transmitter side of the system, the baseband transmitter is implemented with a digital signal processor (DSP) which performs the FEC coding and interleaving on the data symbols, the mapping of symbols to the QAM constellation, the generation of pilot symbols and their mapping to a phase shift keying constellation, the insertion of pilots into the symbol stream, and finally the pulse shaping filter. The intermediate frequency (IF) up-converter is implemented digitally and produces three IF outputs with offset center frequencies which are needed for transmitter antenna diversity. Finally, the radio frequency (RF) up-converter shifts the IF signals to the final carrier frequencies around 220 MHz and drives the three transmit antennas.

On the receiver side of the system, the RF down-converter shifts the received signal to an IF center frequency where the IF down-converter digitally shifts the signal back to baseband. The implementation of the RF down-converter is shown in Figure 2. The remainder of the receiver is the baseband demodulator which is implemented in Signal Processing Workstation (SPW) code. It performs matched filtering, symbol timing synchronization and sampling, frame synchronization, fading channel estimation, de-interleaving, and soft decision FEC decoding. The graphical user interface of the SPW environment is shown in Figure 11.

The use of a programmable DSP in the transmitter and SPW in the receiver streamlined the development, testing, and modification of the sophisticated algorithms implemented in the ITS wireless modem. The system is very flexible and will serve as an ideal testbed for future enhancements. Further details on the system operation are contained in the body of this report.

The wireless modem produced in this project has been thoroughly tested via analysis and bench testing. Field testing has begun and more is planned. In general, the tests performed to date have verified that the modem design performs well, and in fact, the agreement with theory is very close. The laboratory bench testing setup is shown in Figure 22. Three series of bench tests were performed: (1) the baseband demodulator test, (2) the IF test, and (3) the RF test. These tests verified the correct operation of all of the various blocks shown in Figures 9 and 10. The tests allowed for the isolation of problems and the characterization of the entire system. Preliminary field testing was performed by transmitting and receiving inside the MSEE building at Purdue University. These tests including both moving and stationary receivers and the transmitter antenna diversity scheme. More details are contained in the body of the report.

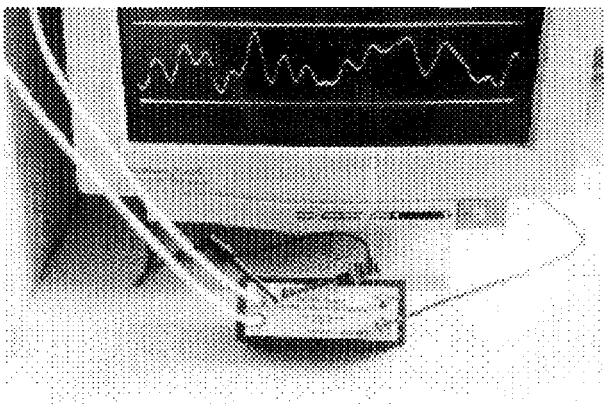

Figure 2: The RF down-converter. The waveform on the monitor is 16 QAM quadrature channel.

We have demonstrated a proof of concept for a general purpose ITS data communication resource. Every aspect of the system works as predicted and our implementation of this modem is quite efficient. Significant work remains to be completed to fully test this system in more realistic environments for ITS applications, but we do not foresee any potential problems. While this implementation does not yet meet the high goal of 3 bps/Hz, this goal can be achieved with fairly minor modifications (a change in the FEC coder/decoder) of the current architecture. This project provides a testbed for future proposed modem improvements or applications of the ITS spectral allocation.

We have had extensive interaction with the Indiana Department of Transportation (INDOT) concerning possible uses for the modem technology developed in this IDEA project in ITS applications and field tests around the state. Some of the promising possibilities include the following:

1. data communications between highway infrastructure and mobile incident response vehicles in INDOT's Borman Expressway Advanced Traffic Management System,
2. transmission of surveillance sensor telemetry to remote concentrators, and

3. multiple access communications in semi-rural adaptive traffic signal coordination.

A proposal to INDOT is pending for funding a project to optimize the wireless modem described in this report for a point-to-point application in remote surveillance camera control. If funded the project will deliver a working digital modem to INDOT with 18,000 bps transmission.

In addition, to our contacts with INDOT we have made many presentations of this work at scientific meetings, to people in the FHWA, and to various industry representatives. Several journal papers describing various aspects of the communication algorithms designed in the project are pending.

INTRODUCTION

Data Communications within ITS

The Federal Highway Administration (FHWA) has identified a set of seven features which form a core infrastructure for the deployment of Intelligent Transportation System (ITS) traffic management and traveler information services in metropolitan areas. The product resulting from this IDEA project addresses a fundamental requirement of all the core infrastructure features: data communication systems linking field equipment with transportation infrastructure. Possible applications of the resulting product will be illustrated with an example in freeway management systems and incident management programs.

ITS Spectral Allocation

In November 1992, five frequency pairs in the 220-222 MHz Land Mobile radio band were allocated to the FHWA for a period of fifteen years. These frequencies will be used by the FHWA in ITS applications which have national implications and benefits, including selected research experiments and operational tests. The frequencies are at 10 kHz spacing with spectral allocation specified as shown in the emission mask plotted in Figure 3. It should be noted from this plot that the usable bandwidth of each channel is roughly 4 kHz.

Given the limited bandwidth (4 kHz) available in the 220 MHz channels, very efficient modems will be required if profitable use is to be made of this resource. Standard twisted-pair telephone circuits also have an available bandwidth of about 3.2 kHz and modem technology has now evolved to the point where transmission rates are at 28.8 kbps for the best twisted-pair lines. This amounts to a spectral efficiency of 9 bps/Hz. The wireless environment is far more hostile, and wireless modems currently available rarely achieve efficiencies greater than 1 bps/Hz. This project focused on providing improved bandwidth efficiencies for narrowband wireless communications with the eventual goal of approaching the efficiency of wireline telephone modems.

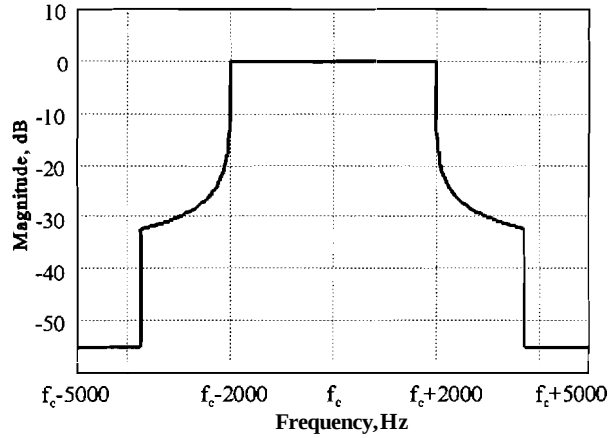

Figure 3: Spectral emission mask for the ITS f_c=220MHz allocations

Narrowband Communications Applications in ITS

ITS application areas which require data communication capabilities between highway infrastructure and mobile vehicles or traffic operations centers include electronic toll collection, automatic vehicle identification, electronic clearance for commercial vehicle operations, traveler information services, and video surveillance. Some of these require fairly large data rates (e.g., electronic toll collection and video surveillance) and, consequently, a larger bandwidth than allowed in the ITS dedicated channels at 220 MHz. Other applications require relatively small data rates, examples of which include vehicle hailing and warning, mayday services, and telemetry transmission from sensors to traffic management centers and incident response vehicles. These are excellent candidates for use of this channel, and high efficiency wireless modems will maximize the utility of this resource.

We have developed a close wor'king relationship with the Indiana Department of Transportation (INDOT) through our collaboration on the Borman Expressway Advanced Traffic Management System (ATMS) and other projects. Having seen many applications for radio technology in INDOT projects, we plan to pursue potential deployments of the proposed wireless modem technology with INDOT.

An Example Application

Communication between the Borman Expressway incident response vehicles (IRV) and the traffic management center is a promising application of the wireless modem developed in this project. The Borman handles approximately 140,000 vehicles per day and is an important link for commercial vehicle operations; roughly 40 percent of the traffic mix consists of large trucks. The major operational problem on the Borman Expressway is non-recurrent congestion due to incidents. Thus, improved incident response is a major component of INDOT's traffic management strategy on the Borman.

INDOT's IRV is a medium duty truck with the capability to clear up minor incidents. The latest generation of IRV is equipped with a 50-foot extendable boom topped by a CCD camera with pan, tilt, and mom control. It has a variety of data communication capabilities including GPS and a laptop computer for recording the specifics of each incident encountered. Due to staffing limitations INDOT envisions the IRV serving as a remote traffic operations center. Therefore, the IRV operator must have the capability to access vehicle detector information, to operate changeable message signs, to operate the highway advisory radio channel and to communicate with other authorities including police, fire, ambulance, and towing services. With the exception of video transmission, the mobile modem technology of this proposal can serve for all of the required communication functions of the IRV.

The Wireless Channel

The services to be provided by ITS are crucial in large cities, where millions of people commute to work daily. Unfortunately, an urban environment coupled with fast-moving vehicles is one of the most hostile scenarios for digital communications. The vehicle motion induces a Doppler shift on the received signal, causing a severe performance degradation in narrowband communications. Reflections from buildings and other vehicles induce multiplicative. multipath distortion which causes frequent deep fades - total blackouts of the received signal.

Figure 4 illustrates a typical land mobile communications scenario. When a single pulse is transmitted from the base station, multiple pulses are received at the mobile unit due to reflections. Each received pulse has a frequency shift (i.e., the Doppler frequency) which is induced by the vehicle speed and angle of incidence of the received.path. In addition, the signal on each path has a different time delay and attenuation due to the path length and reflective coefficient of the obstacles. As the vehicle moves, the delays and attenuations are constantly changing.

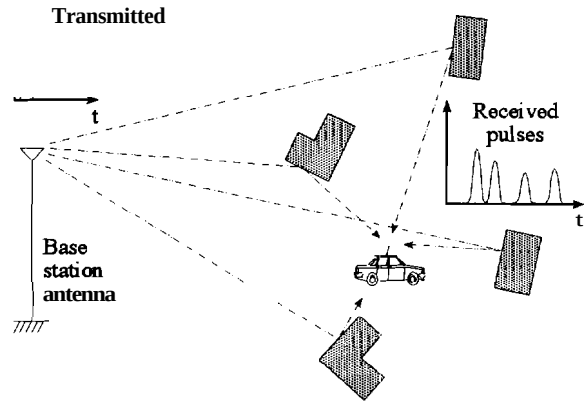

Figure 4: Typical mobile communications scenario

Insight into why the change in delays and attenuations produce rapid signal fading may be gained through the use of the magnitude and phase representation of bandpass signals in Equation 3 of the Appendix. The received signal on the i^{th} path is delayed by τ_i seconds and attenuated by a factor of α_i, and may be written as:

$$r_i(t) = \alpha_i A(t-\tau_i)\cos(2\pi f_c(t-\tau_i) + \theta(t-\tau_i)) = A_i(t)\cos(\theta_i(t)) \quad (1)$$

where f_c is the carrier frequency, $A_i(t) = \alpha_i A(t-\tau_i)$ and $\theta_i(t) = 2\pi f_c(t-\tau_i) + \theta(t-\tau_i)$. Note that the phase $\theta_i(t)$ will be changing much faster than the amplitude $A_i(t)$, because in the phase term the time difference is multiplied by the carrier frequency, which is very large. Figure 5 illustrates this graphically for the case of four received paths. Although the amplitudes of the four received signals are relatively constant in Figures 5(b) and (c), the fading scenario is dramatically different because of the change in phases.

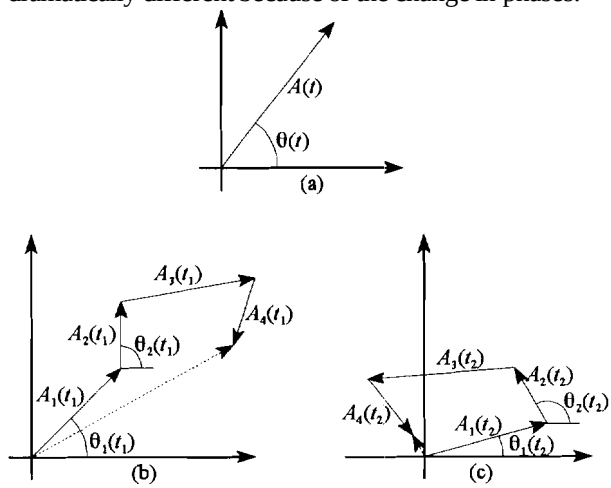

Figure 5: Simplified vector representation of a multipath signal. (a) transmitted signal, (b) received signal at time t_1: strong signal, (c) received signal at time t_2: faded signal.

Experimental measurements and mathematical analysis(*1*) have shown that this results in a signal with frequent deep fades which occur when the phases of the received paths add up destructively. The most severe type of fading is where there is no line of sight path - the entire received signal consists of reflections. This occurs frequently in urban environments and mountainous terrain, and is known as Rayleigh fading. The response of a Rayleigh fading channel to an unmodulated carrier is shown in Figure 1. It is apparent that it will be difficult to transmit information reliably on such a widely fluctuating channel, especially in the instances when the magnitude becomes very small.

For transmitted signals with a carrier fiequency and bandwidth in the ITS spectral allocation and vehicle speeds below 100 mph, the channel fading is relatively constant over several symbol periods. In this case, the channel is accurately represented with the following complex baseband model, as explained in the Appendix:

$$r_n = d_n c_n + n_n \qquad (2)$$

where r_n is the received signal sample,
d_n is the transmitted data symbol,
c_n is the multiplicative channel distortion, and
n_n is additive white Gaussian noise (AWGN).

The data symbol d_n is a complex digital symbol, whereas c_n and n_n are complex valued samples, representing the effects of the channel and noise, respectively. The baseband channel model is depicted graphically in Figure 6.

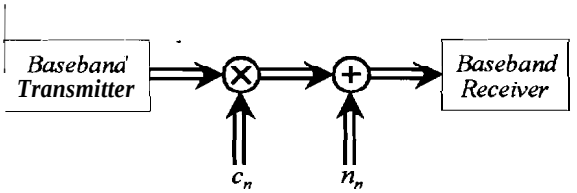

Figure 6: Baseband channel model

Diversity in 'Wireless Transmission

The fading inherent in mobile wireless communication systems severely impairs performance. Figure 7 shows the bit error probability (BEP) of a wireline modem compared to that of a mobile wireless modem' as a function of signal-to-noise ratio (SNR). The BEP is the probability that the receiver incorrectly demodulates a bit due to corruption by the channel and noise. The reason for this reduced performance may be understood by examining Figure 1. Even if the average SNR is large, there are still many times when the instantaneous SNR is quite small. These deep signal fades produce bursts of errors and significantly degrade performance compared to non-fading channels. It is evident that sophisticated algorithms will be required to increase system performance to be commensurate with wireline modems.

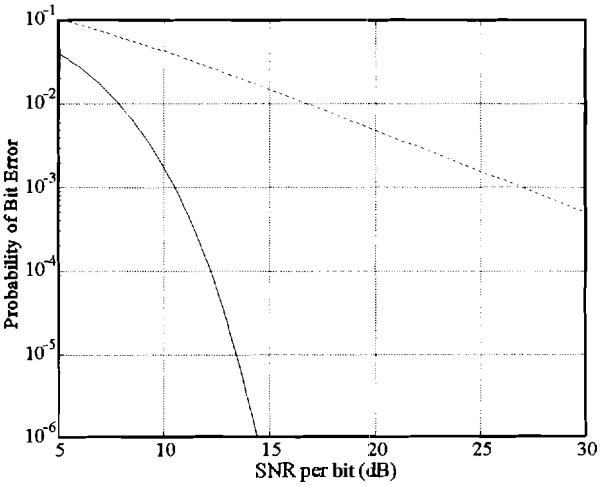

Figure 7: Performance of wireline (solid) versus wireless modem with no diversity (dashed), 16 QAM

The key to improved performance for mobile wireless transmission is diversity(*2*), which involves sending multiple copies of the signal that will suffer independent fading. The idea is that if enough copies are sent, the chances of them all being subjected to a deep fade will be small. Figure 8 shows the improvement in the BEP performance for binary phase shift keying (BPSK) and 16 quadrature amplitude modulation (QAM, described in the Appendix) as the number of diversity levels L_d is increased from one to four. Note that for a given diversity level the BEP performance of BPSK is better than that of 16 QAM. However, it must be remembered that BPSK encotles only one bit per transmitted symbol while 16 QAM encodes four bits per symbol. Therefore 16 QAM is more bandwidth efficient than BPSK and this advantage can overcome the BEP performance disadvantage in a properly designed system.

There are numerous ways to implement diversity in radios, including time diversity, frequency diversity, antenna diversity, or others. An important design issue is ensuring that the fading suffered by each copy of the signal is as near to independent as possible. Effective diversity schemes are based on the fact that the phase on each path is rapidly changing - if the signal copies are designed such that the

[1] This figure was generated assuming zero intersymbol interference, ideal synchronization and channel estimation, and no coding or diversity.

phases of the incoming paths are different, the fading encountered by each copy will be different.

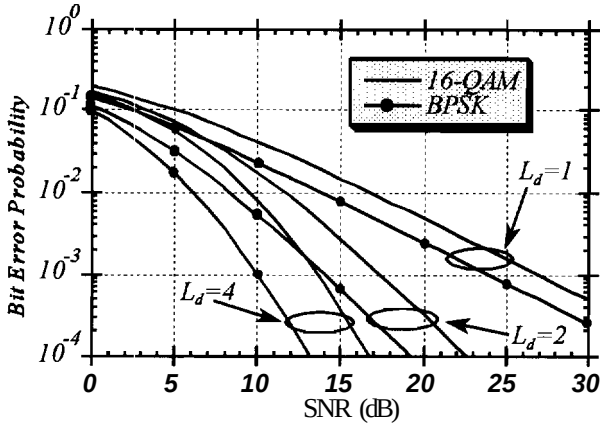

Figure 8: Bit error performance as a function of levels of diversity, L_d

In time diversity, multiple copies of the signal are sent at different times, spaced At apart. Thus, for two levels of diversity, the first copy of the i^{th} received signal will have phase $\theta_i(t)$, and the second copy will have phase $\theta_i(t+\text{At})$. If At is large enough, the phases on each path will be different enough that the fading is independent.

Frequency diversity involves sending copies of the signal on carriers spaced Δf Hz apart, so the phase of the k^{th} copy of the i^{th} received signal (see Equation 1) is $\theta_i(t) = 2\pi(f_c + k\Delta f)(t-\tau_i) + \theta(t-\tau_i)$. If the carrier frequency separation is large enough, the phase characteristics in each band will be independent.

The phase of the received signal is also dependent on the location of the antenna, so by spacing multiple receiver antennas sufficiently far apart, independent fading will result on each received signal. Other types of diversity include antenna polarization, spread spectrum techniques, or angle of arrival diversity.

TABLE 1: !Summary of diversity methods

Diversity Type	Diversity achieved by:
Time	Copies separated by time.
Frequency	Copies separated by frequency.
Antenna	Copies received over independent paths.

All of these methods, summarized in Table 1, have certain drawbacks. In frequency diversity more bandwidth is required, in time diversity the throughput is decreased, and antenna diversity requires more size and weight.

The type of diversity used in this project is a combination of antenna diversity and time diversity. Multiple antennas are used at the base station instead of at the mobile receiver(3),(4). For mobile to base transmission, this is the standard antenna diversity scheme described above. For base station to mobile transmission, which is the link addressed in this project, the diversity scheme is more complicated, although no less effective. Further concepts in communications theory are required to explain this in detail, and will be presented in the remainder of this report.

INNOVATION

The goal of this project was to demonstrate that wireless modems using the ITS spectral allocation can provide a high performance data communication resource. This goal was achieved by implementing a system that brings the performance of land mobile wireless modems closer to that of conventional wireline modems. The major impediment to this goal is the fading environment. Many techniques to mitigate the effects of fading have been developed in recent years, and new algorithms are continually being researched.

Most of this technology is still in the theoretical analysis stage, and few real life systems have implemented all of it. While the best wireline modems achieve efficiencies of about 9 bps/Hz, narrowband wireless modems currently available rarely have efficiencies greater than 1 bps/Hz. This project implements many mobile communications techniques developed in recent years with a goal to achieve about 3 bps/Hz. The design is very flexible so new algorithms can be implemented quite easily to provide even higher efficiency in the future.

The Purdue system incorporates; the following state of the art techniques in digital communications:

- transmitter antenna diversity
- modulation using intentional *frequency* offset
- interleaved block codes
- synchronization optimized *for fading* channeb
- *soft* decision decoding optimized for fading
- pilot symbol assisted modulation
- high order signal *constellations*
- linear equalizer and *matched filter*
- spectrally *efficient pulse* shaping

Many of these techniques have been developed in the 1990's, and the research at Purdue has pushed the state of the art in narrowband wireless data communication. Two Ph.D. theses have been completed in this area(4),(5) and many high quality journal articles have been published on these advanced techniques(6)-(14).

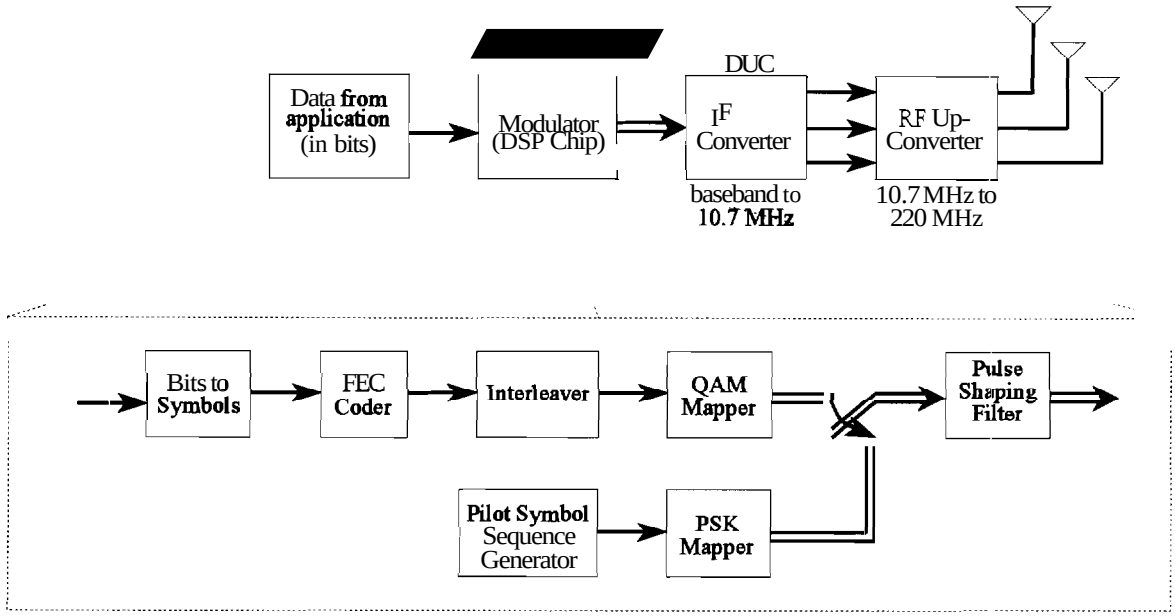

Figure 9: Transmitter Block Diagram

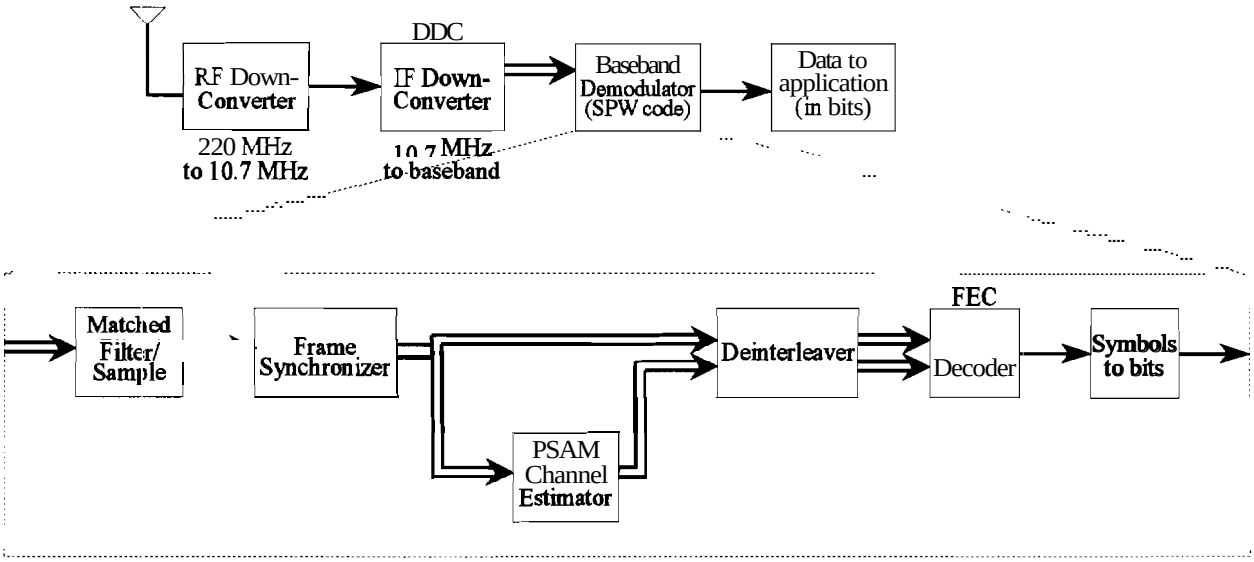

Figure 10: **Receiver** Block Diagram

SYSTEM ARCHITECTURE

A block diagram of the transmitter is shown in Figure 9 and the receiver is shown in Figure 10. In these figures, double arrows denote signals represented in the complex baseband notation, as explained in the Appendix. The baseband modulator and demodulator are implemented in software, enabling future enhancements to be made easily. The baseband modulator is written in assembly language for the Motorola 56002 digital signal processing (DSP) chip. The baseband demodulator is designed using the Signal Processing Worksystem (SPW), seen in Figure 11, a powerful block oriented design program optimized for DSP and communications applications. The final demodulation algorithms can be readily converted to assembly code for implementation on a DSP chip. The digital up-converter (DUC), digital down-converter (DDC) and RF up/down converters are all implemented in hardware. In the following discussion, the operation of each subsystem of the transmitter will be explained along with the con-esponding subsystem at the receiver.

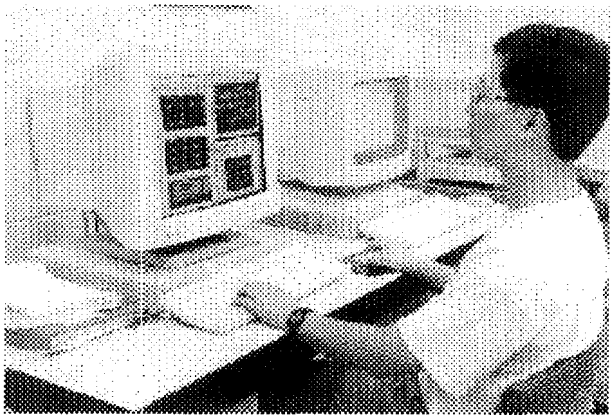

Figure 11: The Signal Processing Worksystem on a Sun Sparc 20

Bits to Symbols/Symbols to Bits

An ITS application needing to transmit digital information sends the information bits to the baseband transmitter. The bit level is the most basic format, so this modem can easily accommodate data fi-om any ITS application. These bits are grouped together in blocks of m bits to form symbols, as explained in the Appendix. Each symbol is a number with value between 0 (all bits zero) and $M-1$ (all bits one, $M=2^m$). At the receiver these symbols will be converted back to bits and passed to the receiving ITS application.

FEC Coder/Decoder

The coder adds redundancy to the message so that it may be transmitted reliably across the channel. Forward error control (FEC) coding(2) allows errors to be detected and corrected at the receiver without any requests for retransmissions. Redundancy is applied by converting K information symbols into a codeword N symbols long, with $N>K$, yielding a code rate of $R = K/N$. An effective coding scheme can greatly improve system performance.

The simplest type of FEC code is a repetition code, in which each symbol (K = 1) is sent N times, thus a codeword is made up of N identical code symbols. A rate 1/3 repetition code was used for testing the system and as a benchmark. Although this simple code has enough error correction capability, it reduces throughput by a factor of 3, so is not suitable for the final system implementation. In order to meet the 3 bps/Hz efficiency goal a higher rate code must be used, which is a straightforward extension.

Interleaver

Note that the coding will be more effective if each symbol of a codeword suffers independent distortion. For example, if a rate 1/3 code were used, and the channel was exactly the same over all three code symbols, the code would have no improvement over an uncoded system. If one of the received symbols was corrupted, they all would be, and nothing would be gained. However, if the channel effect on each code symbol was independent, the probability that all symbols are corrupted would be less than the probability that just one was corrupted, and a coding gain would be realized.

Consecutive samples of the fading channel are correlated, because the multipath scenario changes gradually as the vehicle moves. This may be seen fi-om Figure 1, where the channel gain is relatively smooth for short periods of time. Unless something is done about this correlation, error control coding will have very little ability to compensate for the fading For example, consider again the repetition code of length three - if the three symbols are transmitted consecutively, when a deep fade is encountered all three symbols will be lost, so coding wdl not yield any improvement over an uncoded case.

This problem can be eliminated by shuffling the symbols around so that consecutive code symbols are separated by D_{iv} symbols. This process, referred to as interleaving, is illustrated in Figure 12 for a rate 1/3 repetition code and an interleaver depth, D_{iv}, of 4. The end result of the interleaver is shown in Figure 12(e), where consecutive multiplicative distortion samples for each symbol of the codewords are separated by $D_{iv} = 4$. Provided that the interleaving depth is large enough, all symbols of a codeword will suffer statistically independent fading, because eventually the channel characteristics will change. For very slow fading the required interleaving depth is too large to be implemented. However, it will be shown that transmitter antenna diversity makes it possible to keep D_{iv} small and still achieve robust performance.

QAM Mapper

After the coding and interleaving, the symbols must be mapped to a format suitable for transmission over the channel. QAM is used because of its high bandwidth efficiency. Figure 13 shows the signal constellation for 16 QAM, i.e., QAM with $M = 16$ possible symbols. At each symbol time one of these 16 symbols is transmitted. The channel corrupts the symbol as seen in Figure 14 and the demodulator uses these samples to decide which symbol was sent.

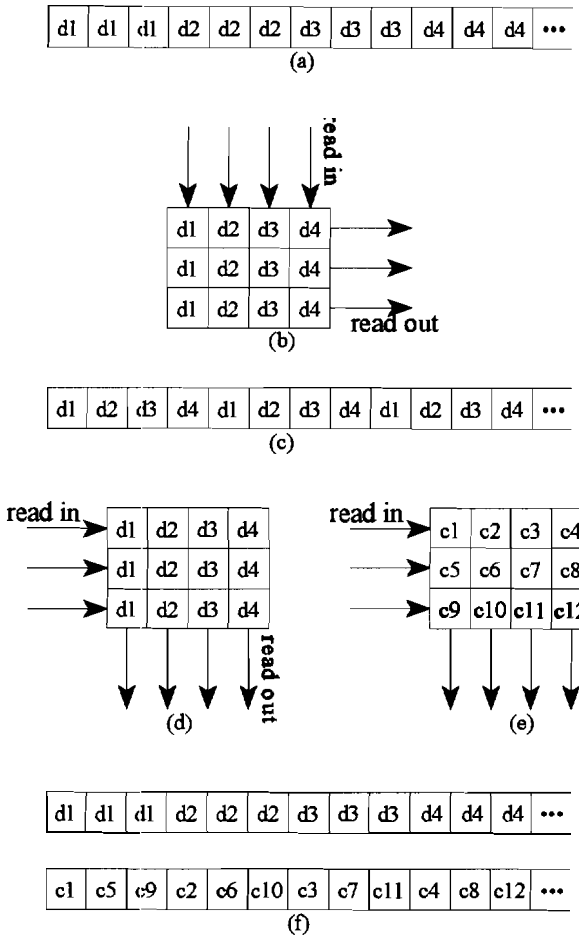

Figure 12: Simplified example of interleaver: rate 1/3 repetition code with D_{iv}=4. (a) The data before interleaving, (b) the interleaving operation, (c) the result of interleaving the data, (d) the de-interleaver operating on the data, (e) the de-interleaver operating on the channel distortion, and (f) the effect of the de-interleaver on the data and channel distortion

Figure 14 shows the received signal constellation, or scatter plot, for 5000 symbols received over an AWGN channel with 20 dB SNR. With this amount of noise, there are still very clear boundaries between symbols, so the error rate will be very small even without sophisticated demodulation techniques. As the noise level increases, the symbols are blurred more, and errors start to become significant.

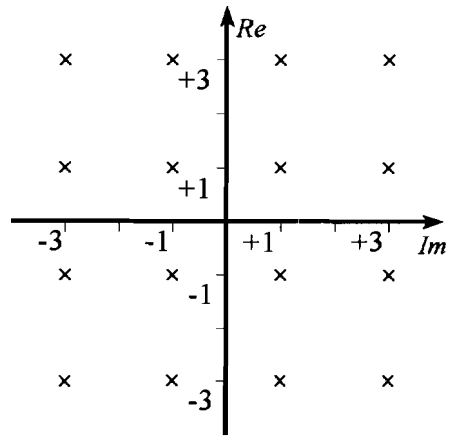

Figure 13: Signal constellation for 16QAM

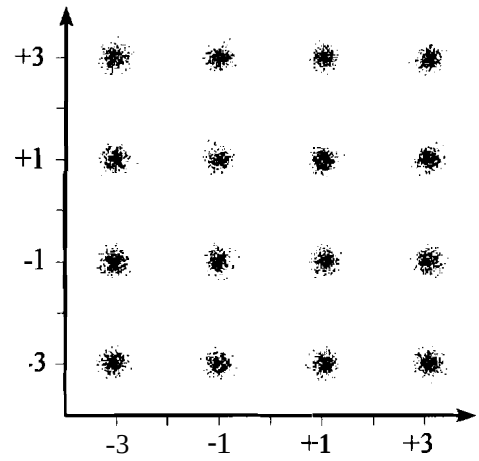

Figure 14: Signal constellation after corruption by AWGN

The received signal constellation resulting from a time-varying Rayleigh fading channel is shown in Figure 15. The fading channel attenuates the signal and rotates the constellation, so the result is extremely distorted. If the fading channel is known exactly and divided out, the result is shown in Figure 16. This result is not as good as in Figure 14 because the Gaussian noise is addled after the fading (see the model in Figure 6). Thus, when the received signal is in a deep fade dividing by the channel will amplify the AWGN, since the channel value is much less than unity. In an actual system, the channel is not known exactly and must be estimated, so the results will be degraded further. However, good channel estimates and FEC coding yield a system that performs well nonetheless.

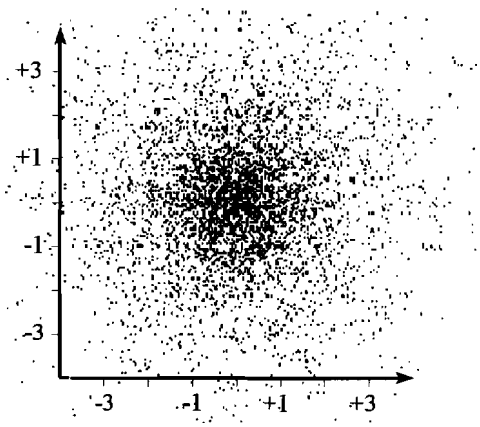

Figure 15: Signal constellation after corruption by Rayleigh fading

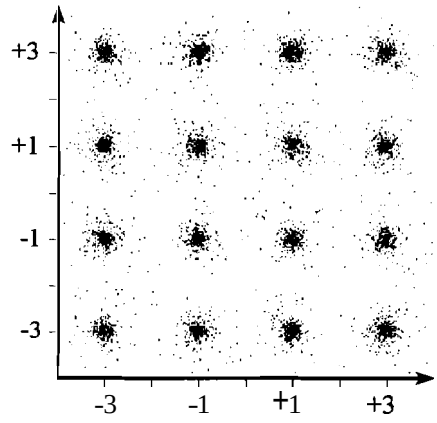

Figure 16: Signal constellation after **channel** estimation has compensated for fading

Pilot Sequence Generator and PSK **Mapper/PSAM** Channel **Estimation**

To obtain an estimate of the fading **channel,** known pilot symbols are inserted periodically into the data stream - this is referred to as pilot symbol assisted modulation (PSAM)(*15*). **The** receiver knows what these symbols are, so by observing how the charnel has corrupted them it can tell how the channel is behaving. The channel may be viewed as a **bandpass** random **process**(*1*), so Nyquist sampling **theory**(*2*) specifies the minimum insertion rate of the pilot **symbols. If pilots** are inserted at or above this rate, it is possible for the **receiver** to reconstruct the channel using a **lowpass** filter. It is well known that the Wiener filter is the linear estimate with minimum mean squared error **from** the actual **channel. Cavers**(*15*) has derived the Wiener **filter** coefficients for the Rayleigh fading channel model shown in Figure 6, and this type of interpolating filter is used in this project. Pilot symbol aided **channel** estimation can track phase variations and small **frequency** offsets of the carrier as well as time-varying fading.

To make the pilot symbols distinguishable from the data symbols, they are chosen **from** a **different** signal constellation. Figure 17 shows the signal constellation of the phase shift keying (PSK) pilot symbols overlaid on the QAM data signal constellation.

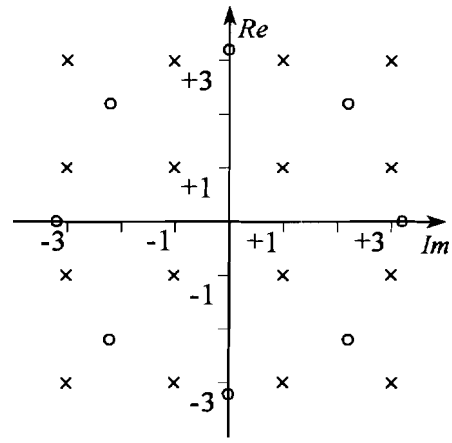

Figure 17: **Constellation** for pilots (circles) overlaid on **16QAM** data (x's)

Pulse Shaping **Filter/Matched** Filter and **Linear** Equalizer

The Federal **Communications** Commission (FCC) spectral mask defines the allowable bandwidth for communications channels. Essentially the spectrum **allocated** to ITS is 4 kHz wide with 500 Hz guardbands on either side, as shown by the solid trace in Figure 18. The transmitter in this project uses a square-root raised cosine pulse shaping **filter**(*2*), **seen** in Figure 18 as the dashed line. It was determined that for this type of filter with a roll-off factor of 15 percent, the maximum **symbol** rate that satisfies the FCC spectral mask is 3571 **symbols** per second.

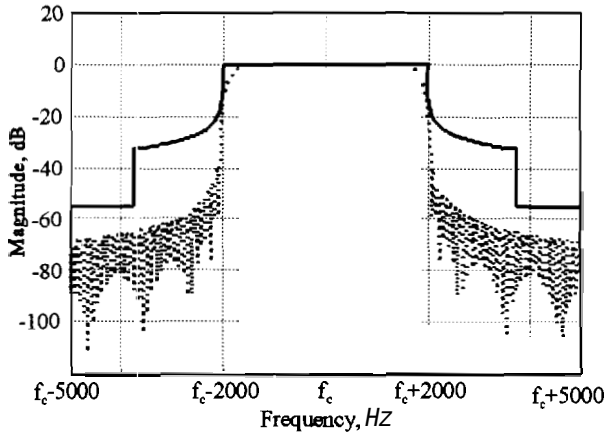

Figure 18: Spectrum of square root raised cosine pulse

IF Up/Down-Converter

The final digital operation of the transmitter is to shift the signal to an intermediate frequency (IF) of 10.7 MHz. Using this IF makes it easy to filter out image frequencies resulting from the up-conversion process. There are three IF outputs, each at a slightly different carrier frequency. This is part of the transmitter antenna diversity scheme, to be discussed shortly.

The IF down conversion is performed digitally to minimize implementation losses. The resulting IF signal (centered at 10.7 MHz) is sampled at 40 MHz and then digitally down-converted to baseband. Figure 19 shows the evaluation boards for the A/D converter and the DDC.

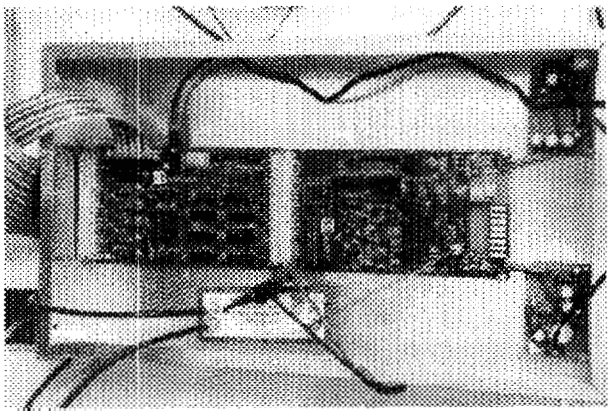

Figure 19: The RF receiver (bottom center) feeds the IF signal to the AID board (right), which sends digital samples to the digital down-converter (left). The baseband diigital signal is fed to a computer where the results are processed using SPW.

RF Up/Down-Converter

The radio frequency (RF) up-converter unit shifts the signal from the IF to the final carrier frequency (220 5825 MHz is the allocation we were given by the FCC) This signal is amplified and filtered to provide the appropnate output power and spectral response to the transmitter antenna. This unit was built with prepackaged subassemblies and may be seen in Figure 20 along with a mobile unit antenna. The RF down-converter provides the necessary frequency conversion, filtering and automatic gam control (AGC) needed to translate the signal from the receiver antenna to an IF frequency with an appropriate power level The AGC can detect a signal from -120 dBm to -40 dBm, and amplifies the output to 0 dBm. The RF receiver is in an integrated subassembly constructed by an outside vendor, and is displayed in Figure 2.

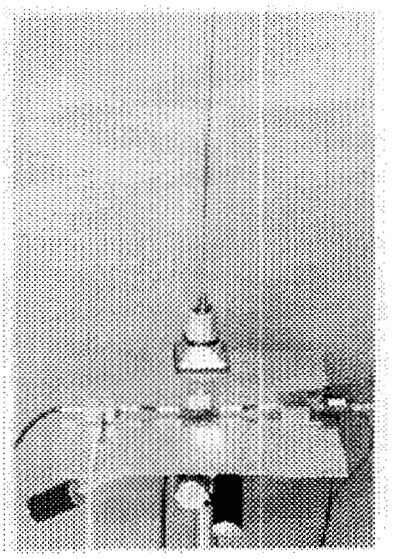

Figure 20: RF transmitter and a receiver antenna.

Transmitter Antenna Diversity

This project implements a form of transmitter diversity in which multiple antennas are used at the base station to achieve the required diversity, and only a single antenna is required at the mobile unit. Each base station antenna uses a slightly different carrier frequency to transmit the signal(*3*). This frequency offset induces a time varying multiplicative distortion which is not dependent on the position of the mobile, as seen in Figure 21. Therefore, when the mobile stops (e.g., at a traffic light) it will still encounter a time varying distortion, and will never be stopped in a deep fade. Since the receiver is already designed to tolerate fading, the addition of another fading process doesn't reduce worst case

system performance. The characteristics of this induced fading process are known and may be used to determine the ideal interleaver depth required to achieve independent distortion on each code symbol(4).

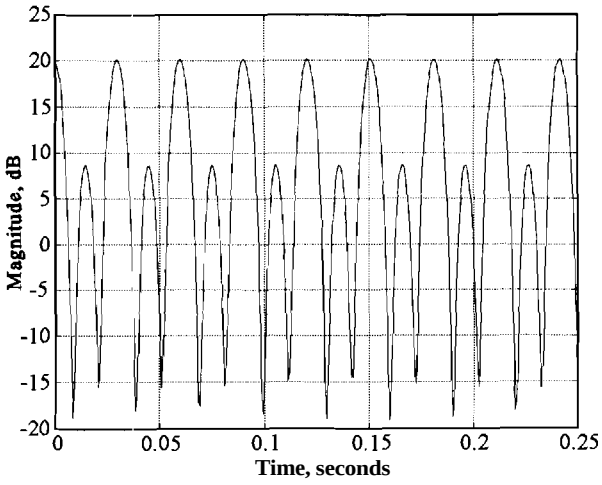

Figure 21: Fading channel response induced by transmitter antenna diversity scheme in a stationary fade

Synchronization

Two different levels of synchronization must be performed in the demodulator before any of the above algorithms will work properly. The first is symbol timing synchronization, which involves finding the best place to sample the received signal to extract the transmitted symbols. This is performed using the digital filter and square algorithm(16), (17) because of its simplicity and tolerance to fading.

Next, frame synchronization determines where the pilot symbols are located among the data symbols. Frame synchronization is also required to insure that the interleaver and the deinterleaver are properly synchronized. This is achieved by passing the received symbol sequence through a weighted correlation filter and threshold detector optimized for the fading channel(6)(18).

BENCH TESTING

A very important part of our program was laboratory bench testing of our transmitter, receiver, modulator, and demodulator. Figure 22 is a picture of our test station in the Communications Research Laboratory at Purdue. This testing shows how close our implementation was to theoretically possible and highlighted the subsystems which need to be improved to achieve even higher spectral efficiencies.

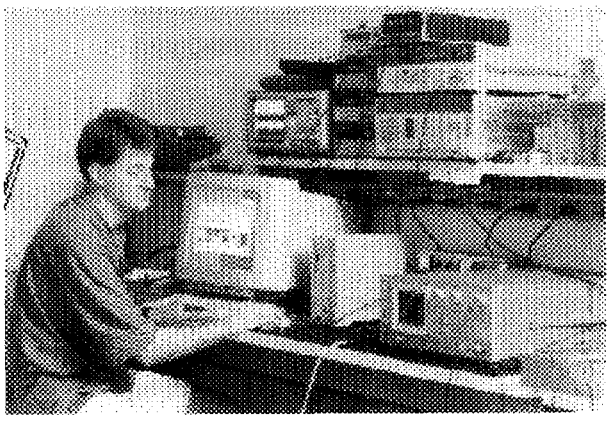

Figure 22: Some of the test equipment in the Communications Research Lab at Purdue

The first set of tests that were run used computer generated data to verify proper operation our baseband demodulator (see Figure 10). The results show that the entire demodulator functioned as expected and all levels of synchronization were achieved (symbol timing, frame timing, and channel estimation.) Figure 23 shows a plot of the BEP as a function of SNR; 26 million bits were passed through the SPW system to generate this curve. It may be seen that the resulting system performance was only 0.5 dB degraded from that theoretically possible, which is typical in communications system implementations.

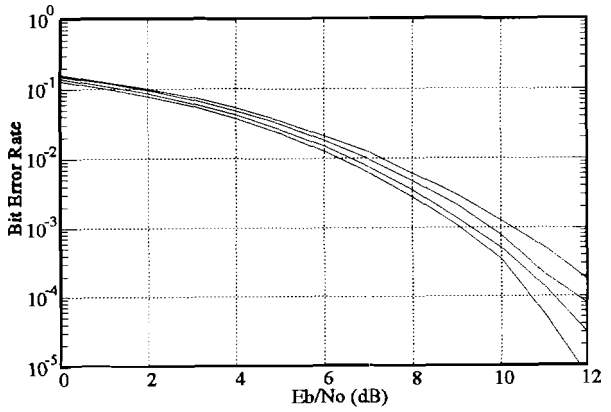

Figure 23: BEP for bench testing subsystems. Leftmost curve is ideal performance, next is SPW generated test data, next is cabled IF data, and the rightmost curve is cabled RF data.

We then tested the system with various levels of hardware integration. This allowed us to isolate problems and fully characterize the entire system. By cabling the IF section to the modulator and democlulator we were able to examine the effects of oscillator mismatch, mode conversion,

and quantization. These effects were in general small as may be seen by the BEP in Figure 23.

Next the RF transmitter hardware was tested in isolation from the rest of the system. This subsystem provided minimal additional degradation and provided an output spectrum (Figure 24) which meets the FCC spectral mask requirement Nonlinearities in the transmitter wmponents can significantly raise the spectral sidebands but the desired output can be achieved with our design.

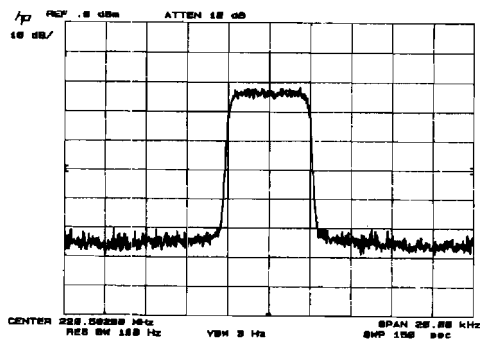

Figure 24: Spectrum of the RF signal as seen on the HP 8568B spectrum analyzer.

The RF transmitter was further tested by demodulating it with test equipment in the Communications Research Lab. The scatter plot in Figure 25 shows that the distortion of the RF transmitter is very small.

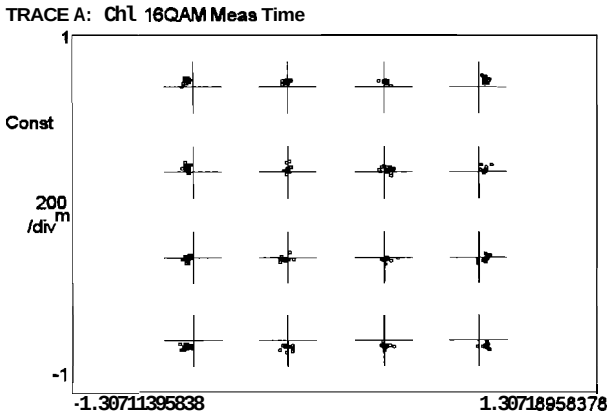

Figure 25: RF 16 QAM signal demodulated with the HP 89441A vector signal analyzer.

The last component tested was the RF receiver unit. Figure 26 shows a scatter plot of the demodulator output for 16 QAM and Figure 23 has the BEP. By comparing Figures 25 and 26 it may be seen that this unit produces significant linear and nonlinear distortions over a fairly significant portion of its operating range. Fortunately the majority of the distortion is for high SNR and at low SNR this unit produces less than 0.5 dB of degradation, as seen from Figure 23. The ISI produced by this receiver unit is significant when we try to push higher bandwidth efficiencies. For example, Figure 27 is a scatter plot of the 64 QAM constellation out of the RF receiver. The 64 QAM constellation points are blurred together much more than for 16 QAM (note that because of the error control coding this trial produced no errors even though the scatter plot seems bad). Further characterization and redesign of this unit is ongoing to enable us to operate at greater bandwidth efficiencies, approaching the quality seen in Figure 25. While the laboratory testing was time consuming because of the large number of tests performed, it was justified because no unexpected results were encountered in the field tests.

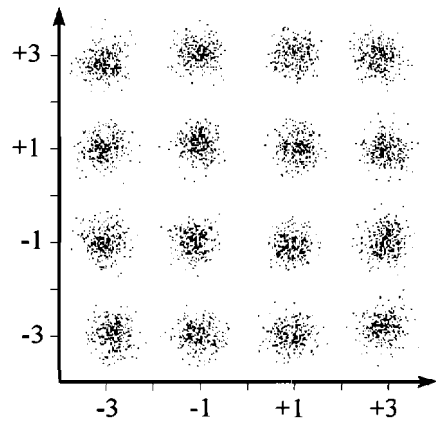

Figure 26: Cabled bench test scatter plot for 16 QAM

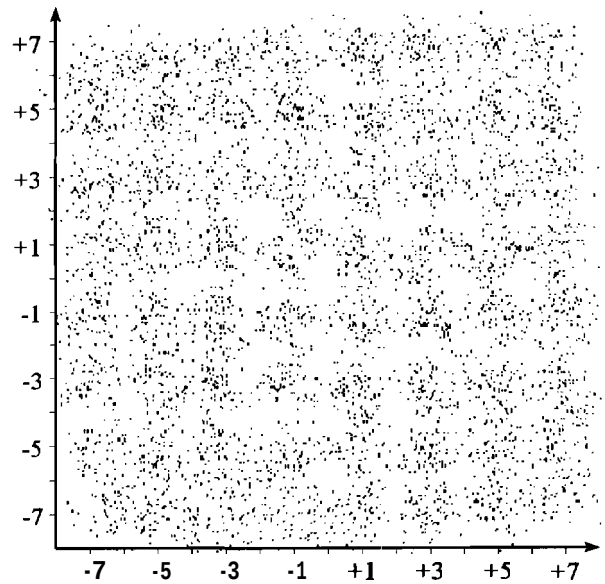

Figure 27 Cabled bench test scatter plot for 64 QAM

FIELD TESTING

Although the field tests up to this point have not been as thorough as originally planned, they have already proven the viability of many of the concepts used in this system. We have been hampered by winter weather because many of our instruments have limited operating temperature ranges, consequently our testing has been confined to indoors. While not entirely the same environment as outdoor vehicular communications, indoor wireless transmission also results in multipath propagation and fading. The transmitter was set up in the Communications Research Laboratory and all tests were performed with the receiver unit within the same building. Since walls provide significant attenuation we were able to test the link over a wide range of received signal power levels. Tests both with the receiver stationary and in motion were performed. We tested BPSK, 16 QAM, and 64 QAM[2] modulations and used single and multiple transmitter antennas. Table 2 documents the tests performed so far.

TABLE 2: Preliminary field testing results

Location	Modulation	Frames Acquired	Bits Acquired	BEP
Stationary test 1 1 antenna	BPSK		8,500	
	16 QAM		37,400	
	64 QAM	68	57,800	
Stationary test 2 1 antenna	BPSK		8,500	
	16 QAM			
	64 QAM	69	58,650	
Stationary test 3 1 antenna	BPSK	10	8,500	0
	16 QAM	45	38,250	0
	64 QAM	68	57,800	
Stationary test 4 1 antenna	BPSK	9	7,650	0
	16 QAM	45	38,250	0
	64 QAM	68	57,800	0
Stationary test 5 1 antenna	BPSK	9	7,650	0
	16 QAM	45	38,250	0
	64 QAM	69	58,650	3.91e-4
Walking test 1 1 antenna	BPSK	19	16,150	0
	16 QAM	90	76,500	3.92e-5
	64 QAM	137	116,450	8.50e-4
Walking test 2 3 antennas	BPSK	20	17,000	0
	16 QAM	90	76,500	2.75e-4
	64 QAM	137	116,450	3.56e-3
Stationary fade test 1 1 antenna	BPSK	20	17,000	0
	16 QAM	90	76,500	2.61e-5
	64 QAM	37	31,450	3.40e-2
Stationary fade test 2 3 antennas	BPSK	20	17,000	0
	16 QAM	90	76,500	9.93e-4
	64 QAM	136	115,600	1.06e-2

The stationary field tests demonstrated a performance much like we saw in the laboratory bench tests. Scatter plots for wireless propagation are seen in Figure 28 and 29 for 16 QAM and 64 QAM respectively. These scatter plots for wireless transmission look much like the scatter plots for the cabled tests (see Figures 26 and 27) which implies that the ISI generated by wireless propagation at these low symbol rates is not significant compared to the ISI generated by the hardware. It will be interesting to see if this conclusion holds when outdoor field tests are run.

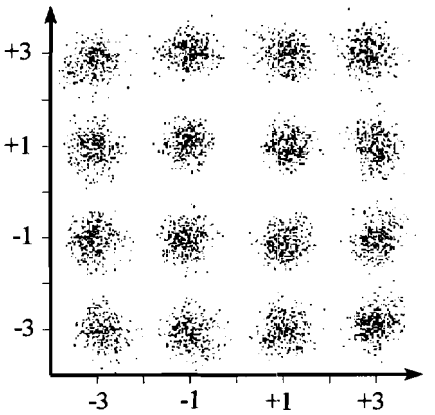

Figure 28: Signal constellation for wireless 16 QAM

[2] With the trivial coding scheme employed for this field test the bandwidth efficiencies were 0.244, 0.974, and 1.46 bps/Hz respectively.

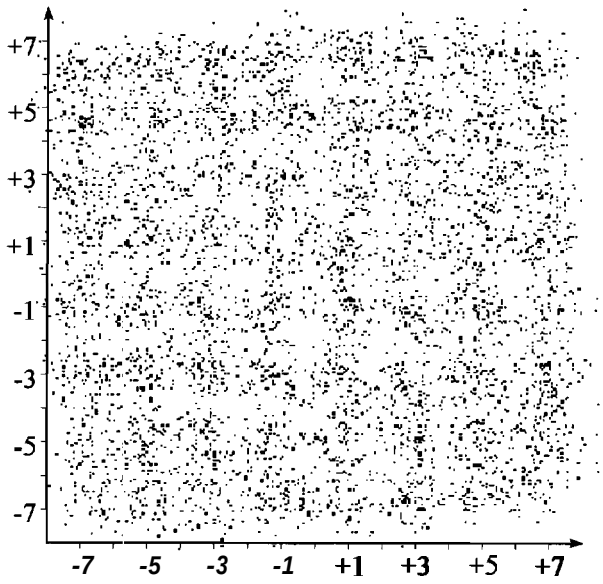

Figure 29: Signal constellation for wireless 64 QAM

Unfortunately we did not fully push the envelope of the link's performance in this set of tests (even though we tried). In the last two tests in Table 2 we positioned the receiver in an apparent deep fade by using the spectrum analyzer to monitor the received signal and moving the receiver antenna around until no signal was evident on the spectrum analyzer. This test location still resulted in a zero or low error rate for most modulations, so apparently our receiver front end is more sensitive than our spectrum analyzer.

Additionally, the transmitter diversity performed as expected. Figure 30 is a plot of the fading induced in a stationary environment with multiple antennas each having a slightly different frequency offset. The fading is quasi-periodic as expected from Figure 21, and after interleaving a maximum of one symbol per codeword is faded as the system was designed(*4*). The 64 QAM signal without the transmitter antenna diversity was severely distorted, and only 37 of 144 transmitted data frames were able to be demodulated When the transmitter diversity system was used at this location the system recognized 136 of the 144 frames and produced a lower error rate[3]. It will be interesting to investigate this scenario in more detail in the future. We will measure the AGC gain to determine where the deep fades are rather than using the spectrum analyzer, because when the spectrum analyzer cannot detect any signal, there are still times when our receiver can demodulate it, even without transmitter antenna diversity.

[3] The remaining frames were not demodulated because they were used to establish frame synchronization.

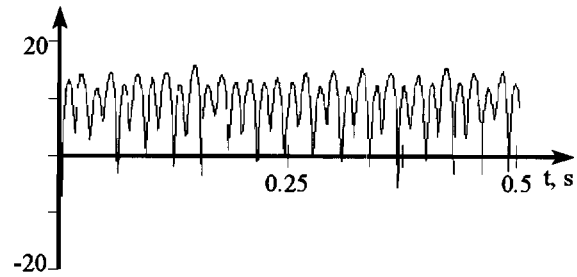

Figure 30: Magnitude in dB ad PSAM estimate of fading channel induced by intentional frequency offset and multiple transmitter antennas.

The mobile tests demonstratecl that system works as theory predicts with time varying clhannel distortion. The mobile tests worked well in general. From Figure 31 it is evident that even at walking speeds significant changes in received signal strength occur in wireless transmission Note that these plots do not have the same types of variations as seen in Figure 1 because the position is changing slowly enough that the AGC in the receiver is compensating for some of the changes in the received signal amplitude.

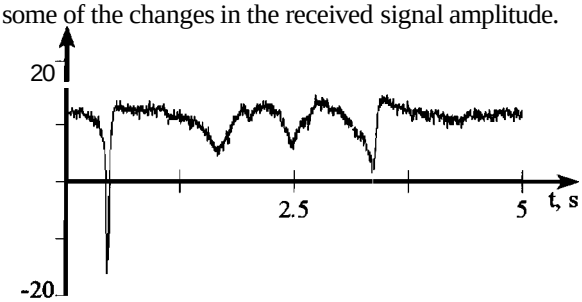

Figure 31: Five seconds of a mobile channel magnitude (single transmitter antenna)

A dramatic example of how well the PSAM channel estimation scheme works in time-varying fading is seen in Figures 32 and 33. Figure 32 shows the scatter plot of the demodulator output for a short time span of a wireless mobile test of 16 QAM data. Comparing this figure to Figure 15 shows that the channel is behaving as predicted in theory and the concentration of the scatter plot around the origin indicates that the signal had a deep fade over the time span plotted. If the scatter plot in Figure 32 is compensated by the channel estimate as was done in Figure 16 then the 16 QAM constellation is again evident. Comparing Figure 33 to Figure 16 demonstrates the demodulator is performing as predicted in theory. This small battery of field tests is merely a *start* toward a full characterization of the link performance, but everything has performed as predicted in theory. A better performance characterization will be available when we can begin outdoor testing later in the spring.

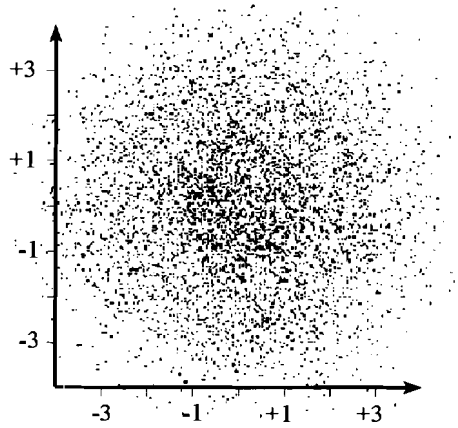

Figure *32:* Constellation of faded **16** QAM signal

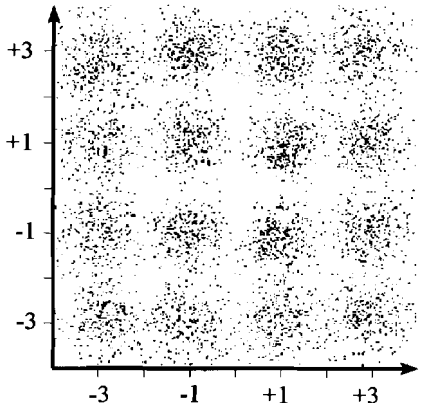

Figure *33:* Constellation of faded **16** QAM signal after channel estimation

CONCLUSION

We have constructed a fully operational end-to-end mobile wireless modem that will achieve 3 bps/Hz efficiency with the minor addition of a higher rate code. This will prove to be a valuable resource for ITS applications. Bench testing and preliminary field tests have been performed, and more thorough field testing is underway.

ACKNOWLEDGMENTS

Many Purdue students have been an invaluable help on this project. We would like to express our appreciation to Jung-Tao Liu, Brett Emsley, Matthew Roos, Marsha Szaniszlo, Rick Wright, Jiann-Ching Guey, Lance Bodnar, and Rob Dyer. A special thanks to Professor J. S. Lehnert for allowing us to use his HP 89441A vector signal analyzer.

APPENDIX: REVIEW OF DATA COMMUNICATION CONCEPTS

Signal Representations of **Bandpass** Signals

Radio frequency communications signals are **bandpass** signals, meaning that their power as a function of frequency is centered around a carrier frequency f_c. Figure 34 illustrates the power spectral density of a typical **bandpass** signal. The bandwidth W of the signal is defined as the maximum minus the minimum frequency where the signal has a significant signal power.

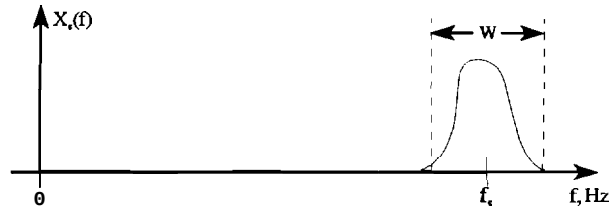

Figure *34:* Typical **bandpass** spectrum

A **bandpass** signal can be written as

$$x_c(t) = A(t)\cos(2\pi f_c t + \theta(t)) \qquad \textbf{(3)}$$

The magnitude of the signal to be transmitted is $A(t)$ and its phase is $\theta(t)$, so a **bandpass** signal has two degrees of freedom. The cosine term is the carrier, and its function is to shift the spectrum from being centered around 0 Hz (baseband) to being centered around f_c Hz (bandpass). This is the process used to provide commercial radio channels - each radio transmission is a **bandpass** signal with a carrier frequency and bandwidth specified by the FCC.

An equivalent and often useful representation of a **bandpass** signal is the in-phase and quadrature representation:

$$x_c(t) = x_I(t)\cos(2\pi f_c t) - x_Q(t)\sin(2\pi f_c t) \qquad \textbf{(4)}$$

The signals $x_I(t)$ and $x_Q(t)$ are usually denoted the in-phase and quadrature components of the signal, respectively. The **bandpass** signal still has two degrees of fieedom; now they are $x_I(t)$ and $x_Q(t)$ instead of $A(t)$ and $\theta(t)$. It is easy to convert to or from the magnitude and phase representation of Equation 3 via the elementary trigonometric transformation:

$$A(t) = \sqrt{x_I(t)^2 + x_Q(t)^2} \qquad \theta(t) = \tan^{-1}\left(\frac{x_Q(t)}{x_I(t)}\right) \qquad \textbf{(5)}$$

$$x_I(t) = A(t)\cos(\theta(t)) \qquad x_Q(t) = A(t)\sin(\theta(t))$$

Since bandpass signals have two degrees of freedom, they may be represented using a complex number or a two-dimensional vector. This notation is known as the complex baseband representation, since the carrier term is omitted, and is written as

$$z(t) = x_I(t) + j x_Q(t) \quad (6)$$

Note that the real part and the imaginary part of a complex number are 90 degrees from each other and are orthogonal, just as the sine and cosine are. This is the basis for the complex baseband representation.

Data Communications

Digital signals are made up of bits, and the first task of transmission is to map them into more bandwidth efficient symbols. Blocks of m bits are grouped together to make one symbol out of a set of $M = 2^m$ symbols. For example, if the bits are grouped in pairs, there are $2^2 = 4$ possible combinations. One such mapping is called pulse amplitude modulation (PAM) and is shown in Figure 35. This type of plot is called a signal constellation, or scatter plot, and is a plot of the entire symbol set.

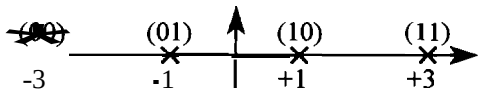

Figure 35: Mapping from bits to digital symbols - 4 PAM

Figure 36 depicts the entire digital modulation process. An example bit stream is shown in Figure 36(a), and the corresponding digital PAM symbols are in Figure 36(b). These symbols are plotted in Figure 36(c), where it may be seen that a new symbol is transmitted every T seconds. The square pulse shape has infinite bandwidth, so the symbols must be shaped with a more efficient filter as shown in Figure 36(d). Finally, the signal is multiplied by the carrier as in Equation 4 to generate the bandpass signal.

In general, the baseband signal may be a complex signal in which case a PAM mapping would be performed in both the real and imaginary parts. This type of modulation has higher bandwidth efficiency, and is known as quadrature amplitude modulation (QAM).

LIST OF ACRONYMS

A/D	analog to digital
ATMS	Advanced Traffic Management System
AWGN	additive white Gaussian noise
BEP	bit error probability
bps	bits per second
BPSK	binary phase shift keying
CCD	charge coupled device
CRL	communications research lab at Purdue University
D/A	digital to analog
DDC	digital down-converter
DSP	digital signal processor
DUC	digital up-converter
FCC	Federal Communications Commission
FEC	forward error control
FHWA	Federal Highway Administration
GPS	Global Positioning System
IDEA	Innovations Deserving Exploratory Analysis
IF	intermediate frequency
INDOT	Indiana Department of Transportation
IRV	incident response vehicle
ITS	Intelligent Transportation System
PSAM	pilot symbol assisted modulation
PSK	phase shift keying
QAM	quadrature amplitude modlulation
RF	radio frequency
SPW	Signal Processing Worksystem

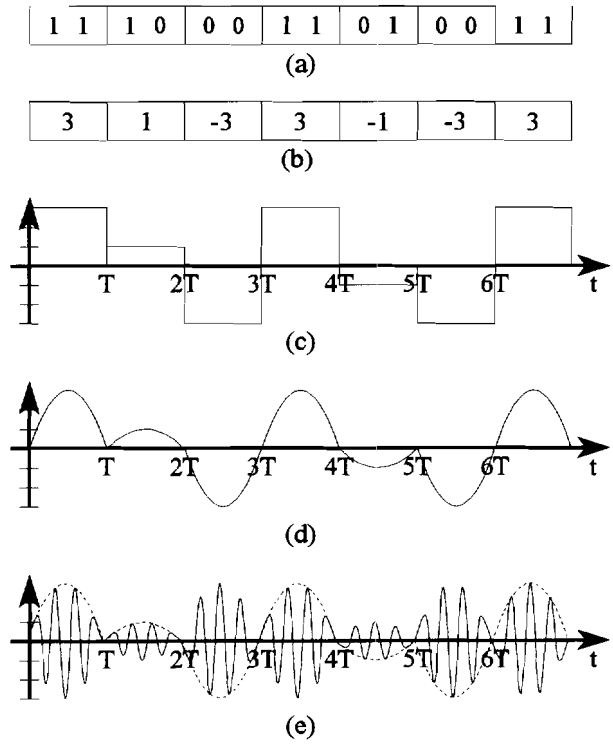

Figure 36: Digital modulation process. (a) bits to be transmitted, (b) bits converted symbols, (c) digital waveform, (d) pulse shaped waveform, (e) bandpass signal

REFERENCES

1. W. C. Jakes, ***Microwave Mobile Communicatiom,*** Wiley, New York, 1974.

2. J. G. Proakis, ***Digital Communicatiom,*** McGraw-Hill, New York, 1995.

3. A. Hiroike, F. Adachi, and N. Nakajima, "Combined Effects of Phase Sweeping Transmitter Diversity and Channel Coding," IEEE Trans. Veh. Tech., VT-41, May 1992, pp. 170-176.

4. W. Y. Kuo, "Architecture Designs for Improving Performance in Fading Channel Communications," Purdue University, 1994.

5. J. P. Seymour, "Improved Synchronization in the Mobile Communications Environment," Purdue University, 1994.

6. J. A. Gansman, M. P. Fitz, and J. V. Krogmeier, "Optimal and Suboptimal Frame Synchronization for Pilot Symbol Assisted Modulation," submitted to the IEEE Trans. Com.

7. M. P. Fitz and J. P. Seymour, "A Principled Framework for Narrowband Mobile Digital Communications," in Wireless Personal Communications - Research Developments, edited by B.D. Woemer, T.S. Rappaport, J.H. Reed, pp 107-118, Kluwer Academic Publishers, 1995.

8. W. Y. Kuo and M. P. Fitz, "Frequency Offset Compensation in Frequency Flat Fading," accepted pending revision to the IEEE Trans. Com.

9. W. Y. Kuo and M. P. Fitz, "Design and Analysis of Transmitter Diversity Using Intentional Frequency Offset for Wireless Communications," submitted to IEEE Trans. Veh. Tech.

10. J. C. Guey, M. P. Fitz, M.R. Bell, and W. Y. Kuo, "Signal Design for Transmitter Diversity Wireless Communication Systems Over Rayleigh Fading Channels," submitted to the IEEE Trans. Com.

11. J. P. Seymour and M. P. Fitz, "Near-Optimal Symbol-by-Symbol Detection Schemes for Flat Rayleigh Fading," IEEE Trans. Commun., vol. COM-43, February 1995, pp. 1525-1533.

12. W. Y. Kuo and M. P. Fitz, "User Slot Design and Performance Analysis for Burst Mode: Communication with Fading and Frequency Uncertainty," International Journal on Wireless Information Networks, vol. 1, October 1994, pp. 239-252.

13. J. P. Seymour and M. P. Fitz, "Two-Stage Camer Synchronization Techniques for Flat Fading," IEEE Trans. Veh. Technol., vol. VT-44, February 1995, pp. 103-110.

14. M. P. Fitz and J. P. Seymour, "On the Bit Error Probability of QAM Modulation," International Journal on Wireless Information Networks, vol. 1, April 1994, pp. 131-139.

15. J. K. Cavers, "An Analysis of Pilot Symbol Assisted Modulation for Rayleigh Faded Channels," IEEE Trans. Veh. Technol., vol. VT-40, November 1991, pp. 686-693.

16. E. A. Lee and D. G. Messerschmitt, ***Digital Communications***, Kluwer Academic Publishers, Boston, 1988.

17. M. Oerder and H. Meyr, "Digital Filter and Square Timing Recovery," IEEE Trans. Commun., vol. COM-36, May 1988, pp. 1988.

18. J. A. Gansman, M. P. Fitz, and J. V. Krogmeier, "Frame Synchronization for Pilot Symlbol Assisted Modulation", Proceedings 33rd Allerton Conference on Communications, Control, and Computing, Oct. 1995.